



Technical Note

Burnup-Dependent Neutron Spectrum Behaviour of a Pressurised Water Reactor Fuel Assembly

Bright Madinka Mweetwa¹ and Marat Margulis^{1,2,*}

¹ Nuclear Futures Institute, Bangor University, Dean Str., Gwynedd, Bangor LL57 1UT, UK; brm22kcj@bangor.ac.uk

² College of Science and Engineering, University of Derby, Kedleston Rd., Derby DE22 1GB, UK

* Correspondence: m.margulis@derby.ac.uk

Abstract: Understanding the behaviour of a neutron spectrum with burnup is important for describing various phenomena associated with reactor operation. The quest to understand the neutron spectrum comes with a lot of questions. One question that is usually asked by students is: Does the neutron spectrum harden or soften with burnup? Most textbooks used by students do not provide a definite answer to this question. This paper seeks to answer this question using a 3D model of a standard 17×17 pressurised water reactor fuel assembly. Two cases were studied using the Serpent Monte Carlo code: the first considered the fuel assembly with constant boron concentration (traditionally found in many published papers), and the second considered boron iteration (where the boron concentration was reduced with burnup). Neutron spectra for the two cases at beginning of life and end of life were compared for spectral shifts. In addition, thermal spectral indices were used to assess spectrum hardening or softening with burnup. Spectral shifts to lower energies were observed in the thermal region of the neutron spectrum, whereas the fast region experienced no spectral shift. There was an increase in thermal spectral indices indicating that the spectrum became soft with burnup.

Keywords: absorption heating; diffusion cooling; spectrum hardening; spectral indices; linear reactivity model



Citation: Mweetwa, B.M.; Margulis, M. Burnup-Dependent Neutron Spectrum Behaviour of a Pressurised Water Reactor Fuel Assembly. *J. Nucl. Eng.* **2024**, *5*, 44–56. <https://doi.org/10.3390/jne5010004>

Academic Editor: Dan G. Cacuci

Received: 15 December 2023

Revised: 18 January 2024

Accepted: 22 January 2024

Published: 29 January 2024



Copyright: © 2024 by the authors. Licensee MDPI, Basel, Switzerland. This article is an open access article distributed under the terms and conditions of the Creative Commons Attribution (CC BY) license (<https://creativecommons.org/licenses/by/4.0/>).

1. Introduction

Neutrons are fundamental to the operations of nuclear reactors, and their behaviour in different reactor configurations has been an ongoing topic of research and discussion since the dawn of nuclear energy in the 1960s. The behaviour of the neutron spectrum from the beginning of life (BOL) to the end of life (EOL) of a fuel assembly in a reactor is influenced by several factors [1]. These factors include fuel type, reactor core materials, core configuration, and irradiation time. As a reactor operates and fuel depletes, many nuclides are produced as fission products [2]. These nuclides are produced through fission, transmutation, and the decay of unstable radionuclides. The nuclide inventory depends on the initial fuel composition, neutron flux spectrum and intensity, and burnup [3].

The neutron flux spectrum is an important parameter required to predict the fuel's behaviour as a function of time. Many parameters influence its behaviour, as mentioned above. The fission product inventory substantially impacts the thermal utilisation factor, affecting the neutron spectrum behaviour [4]. High concentrations of nuclides with high neutron absorption cross-sections negatively affect the reactor's thermal utilisation factor, neutron multiplication, and reactivity [5]. Among the fission products of concern are Xe-135 and Sm-149, as their concentrations can change during transients and impact the neutron population and spectrum [6]. The presence of boron in the coolant and its programmed change in concentration with burnup combined with load follow transients as well as presence of voids, causes alternation in the neutron flux and the spectrum [7]. In addition,

the production of fissile trans-uranium isotopes, such as Pu-239, Pu-241, and Am-242 m, contributes to the core’s neutron population increase [8]. The net effect of neutron poison and fissile isotopes on the neutron spectrum at EOL in light water reactors (LWR) has been discussed among reactor physicists and nuclear engineers.

Thus, a question arises:

Does the neutron spectrum in a PWR soften or harden with burnup?

This question is common among students starting their carrier in nuclear engineering. Surprisingly, none of the textbooks commonly used by students provide a definitive answer [9,10]. Outside of traditional textbooks, discussions among experts in the field are characterised by divergent views with opinions split between hardening and softening of the spectrum. Several studies have covered neutron spectrum hardening and softening as it relates to burnable absorber-doped fuel and other reactor transients. For example, Galahom [11] mentions neutron spectrum hardening in relation to the use of burnable absorbers and, in an IAEA Techdoc [12], it is discussed in the context of extended burnup. However, not much work has been covered that primarily focuses on the status of the neutron spectrum with respect to hardening or softening at EOL. In addition, many studies that mention spectrum hardening or softening are based on 2D fuel assembly models and do not consider leakage or boron letdown with burnup, which significantly affects the conclusion [13]. This paper evaluates behaviour of a neutron spectrum with burnup for a single PWR fuel assembly and seeks to provide an answer to this recurring question.

2. Theory

Neutrons are born at high kinetic energies in the range of 0.1 MeV to 10 MeV with an average energy of 2 MeV. The fission spectrum can be expressed by Equation (1) [14].

$$\Phi(E) = v \cdot n_0 X(E) = \sqrt{\frac{2E}{m}} \cdot n_0 \cdot 0.453 \cdot e^{-1.036E} \cdot \sinh(\sqrt{2.29E}) \tag{1}$$

where v is the kinetic energy of neutrons, n_0 is the number of neutrons, and m is the mass of the neutron.

The neutron spectrum in a typical pressurised water reactor (PWR) has an energy range of 0.025 eV–10 MeV [15]. As a result of the varying neutron energies, the spectrum is usually classified into three energy regions; namely, the fast region with a range of 10 MeV–1 keV, the epi-thermal (resonance region) with a range of 1 keV–1 eV, and the thermal region with a range of 1 eV–0.025 eV.

Fast neutrons undergo various interactions with moderator materials to reach thermal energies. At high energies, elastic and inelastic scattering dominates the slowing down of neutrons, whereas the epi-thermal region is dominated by resonance absorption. The thermal region is dominated by up-scattering as most neutrons are almost in thermal equilibrium with reactor materials. When neutrons have slowed down to thermal energies, their energy distribution is well defined by the Maxwell–Boltzmann distribution as presented by Equation (2).

$$M(E) = \frac{2\pi n_0}{(\pi kT)^{3/2}} \cdot E^{1/2} \cdot e^{-E/kT} \tag{2}$$

where n_0 is the number of neutrons per unit volume (total neutron density), k is Boltzmann’s constant, and T is the absolute temperature in Kelvin. Equation (3) shows the thermal neutron flux density

$$\Phi(E) = v \cdot n_0 \cdot M(E) = \sqrt{\frac{2E}{m}} \cdot n_0 \cdot \frac{2\pi E^{1/2}}{mkT^{3/2}} \cdot e^{-E/kT} \tag{3}$$

where v is the kinetic energy of neutrons, n_0 is the number of neutrons, m is the mass of the neutron and $M(E)$ is the Maxwellian distribution, k is Boltzmann’s constant, and T is the absolute temperature in Kelvin [16].

Neutron Spectrum Perturbation

The equilibrium thermal spectrum presented by Equation (3) can be perturbed primarily in four ways. These are *absorption heating*, *diffusion cooling*, *slowing down source*, and through *thermal resonances*. *Absorption heating* occurs when the equilibrium thermal spectrum shifts to higher energies due to the introduction of a thermal neutron-absorbing medium. A shift to higher energies of a neutron spectrum is generally referred to as spectrum hardening. For a finite system where leakage cannot be neglected, the introduction of a leakage term in Equation (3) will cause the spectrum to shift to lower energies [17].

Going from an infinite system to a finite system introduces leakage. Fast neutrons, with a larger mean free path, are more likely to leak than thermal neutrons. Hence, finite systems have softer spectra than their equivalent infinite systems. The shift in the thermal spectrum to lower energies due to leakage is referred to as '*diffusion cooling*'.

In the *slowing down source* case, there is a constant source of neutrons slowing down from the epi-thermal region. These neutrons are affected by the $1/\sqrt{E}$ effect, where the cross-section increases with reducing energy. The increase in cross-section leads to increased absorption of neutrons with lower energies. This causes a build-up of neutrons with slightly higher energies within the thermal region. A build-up of these neutrons causes an upward tilt and shift to higher energies of the equilibrium thermal spectrum around the thermal–epithermal boundary.

Perturbation of the equilibrium thermal spectrum due to *thermal resonances* is caused by the presence of heavy nuclides such as U-235 and Pu-239, which have high resonances in the thermal region of the spectrum. These distort the thermal spectrum shape. This effect is more pronounced towards the EOL of a reactor with low enrichment [18].

3. Materials and Methods

A standard 17×17 Westinghouse Pressurised Water Reactor (PWR) fuel assembly was used for the study. A 3D fuel assembly was modelled using the Serpent Monte Carlo code. Figure 1 show the 3D fuel assembly lattice model. The parameters used to model the fuel assembly are provided in Table 1.

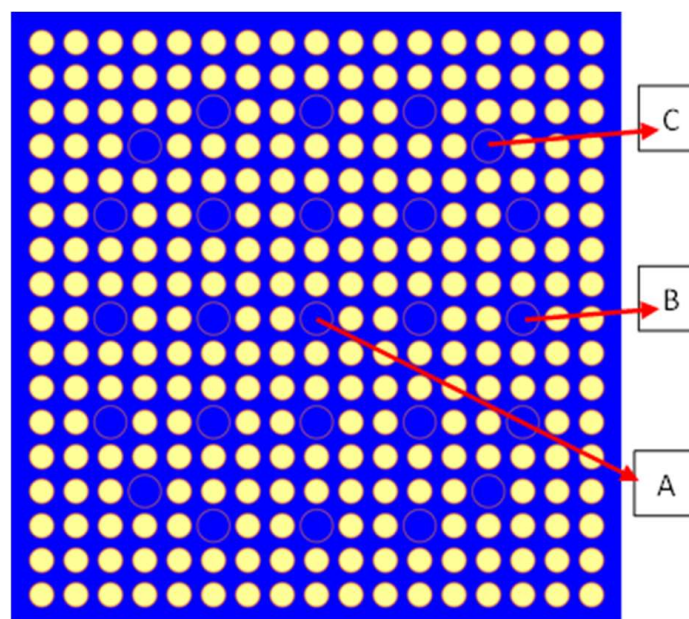


Figure 1. Lattice model for the 3D fuel assembly.

Table 1. Geometry and Parameters for Fuel Assembly.

Parameter	Value
Fuel rod lattice arrangement	17×17
Active fuel length (cm)	426.7
Thickness of reflector (cm)	30.0
Fuel radius (cm)	0.447
Natural Zr clad radius (cm)	0.513
Pitch step (cm)	1.26
Fuel temperature, (K)	900
Natural Zr clad and moderator temperature, (K)	600
Fuel enrichment (wt%)	4.5
Fuel density (g/cm^3)	10.745
Moderator density (g/cm^3)	0.74
Average power density, (W/g)	40
Detector radius and length dimensions (cm)	0.630×426.7

A cuboid was used to define the finite 3D fuel assembly model with reflective boundary conditions in the 'x' and 'y' directions and black boundary in the 'z' direction.

Two simulation cases based on the model described in Table 1 were run using the Serpent Monte Carlo code with ENDF/B-VII.0 cross-section libraries [19,20]. The neutron population was set at 400,000, with the inactive and active cycles set at 500 and 20, respectively. The WIMS172 energy group structure was used to estimate the neutron spectrum. Burnup calculations were set for the range 0 MWd/kg to 60 MWd/kg.

Case 1: The boron iteration card was invoked. The card was used to perform a critical boron search, determine the EOL for the fuel assembly, and to give an indication of the boron concentration at each burnup step. The initial boron concentration was set at 1000 ppm.

Case 2: The boron concentration was kept constant at 1000 ppm. This was carried out to study the effect of boron on the neutron spectrum at BOL up to EOL and for comparison of the results with the boron iteration case.

For each of the cases, the following simulations were performed.

1. Miniature fission chamber detectors were modelled and inserted into fuel assembly guide tubes at locations A, B, and C, as shown in Figure 1. The dimensions for detectors are provided in Table 1. The detectors were used to calculate fission and capture reaction rates for U-235, U-238, and Pu-239. This was carried out to maintain a realistic representation of detectors as used in a reactor core;
2. The fuel assembly described in (1) was divided into 20 axial segments, with each segment having an axial length of 21.335 cm. The detectors in each of the segment was used to score the fission and capture reaction rates for U-235, U-238, and Pu-239. The average for two middle segments (one from the top part of the assembly and the other from the bottom part of the assembly) were used to calculate the capture reaction rates for U-235, U-238, and Pu-239, and the associated spectral indices. This approach was adopted to observe the behaviour of the spectral indices in the middle part of the assembly, which has high burnup;
3. The entire fuel assembly model was treated as a detector with the fission and capture reaction rates for U-235, U-238 and Pu-239 in the fuel used to calculate the spectral indices.

4. Results

4.1. Data Processing

The boron concentration at each burn step for the boron iteration case (Case-1) was obtained by multiplying the burn step iteration factor with the value of the initial boron concentration guess used in Case-1 input file. The concentrations were then plotted against the corresponding burnup step to obtain the boron let-down curve. The let-down curve

gives an indication of the boron concentration required (at each burnup step) to hold down excess reactivity in such a way as to keep the reactor critical. The EOL was determined when criticality dropped below unit (1) and the corresponding boron concentration was found to be 60 ppm. The boron let-down curve for Case-1 is presented in Figure 2. The figure also shows the variation in reactivity with burnup for the constant boron case (Case-2). The EOL for the constant boron was determined using the linear reactivity model (LRM) which assumes that the fuel assembly would be loaded in a core that applied a three (3)-batch loading scheme. The burnup B1, 2B1, and 3B1 in Figure 2 indicate the assumed three cycles for the core. Thus, the EOL for the constant boron case would be at 3B1. Figure 3 shows neutron spectra at BOL and EOL for the fuel assembly model for cases 1 and 2.

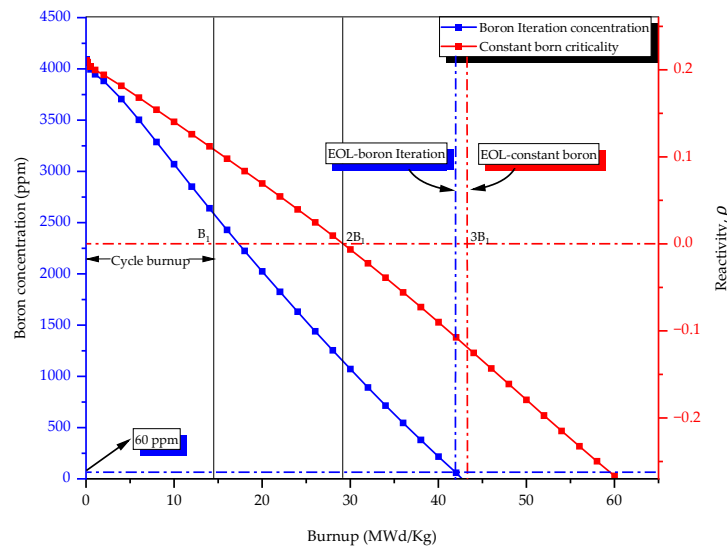


Figure 2. Boron let-down curve and constant boron criticality variation with burnup.

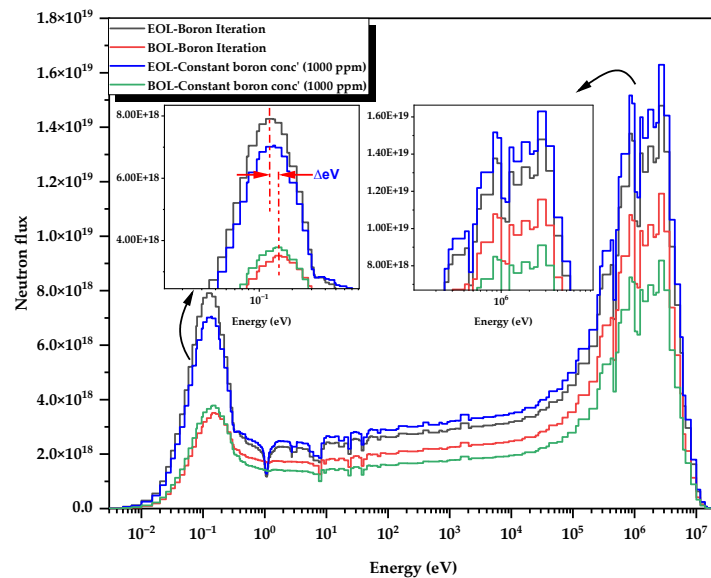


Figure 3. Comparison of neutron energy spectra for boron iteration and constant boron at BOL and EOL.

To assess the neutron spectrum, fast and thermal spectral indices were used. Fast spectral indices are a ratio of U-238 fission to U-238 capture reaction rates. Because U-238 fission has a threshold reaction at around 1 MeV, an increase in this index will indicate if there has been a shift of the fast peak component of the spectrum to higher energies. In this

paper, the fast spectral indices are denoted as $U8fis/U8cap$. The spectral indices for the middle segment of the fuel assembly are denoted as $U8fis/U8cap-mid$. An increase in the fast spectral index indicates an increase in the fast component of the neutron spectrum.

Thermal spectral indices are a ratio of the U-235 or Pu-239 fission reaction rate to U-238 capture reaction rates which, in this paper, are denoted as $U5fis/U8cap$ and $P9fis/U8cap$, respectively. An increase in thermal spectral indices with burnup indicates neutron spectrum softening, and a decrease indicates spectrum hardening [21].

The fission and capture reaction rates for each of the isotopes (U-235, U-238, and Pu-239) were scored as described in Section 3. For each of the cases, fast and thermal spectral indices were calculated for each burnup step from 0 MWd/kg to 60 MWd/kg. This was carried out for the boron iteration and constant boron cases with reference to locations A, B, and C as shown in Figure 1 as well as for the simulation with the entire assembly treated as a detector. Thermal spectral indices were plotted against burnup as presented in Figures 4 and 5. To further analyse the behaviour of these spectral indices, the reaction rates were normalised to unit, and the resultant plots are presented in Figures 6–8. Figures 9 and 10 compare the fast spectral indices for the full assembly treated as a detector and those of the mid-assembly axial segment. These figures are further analysed in Figures 11 and 12.

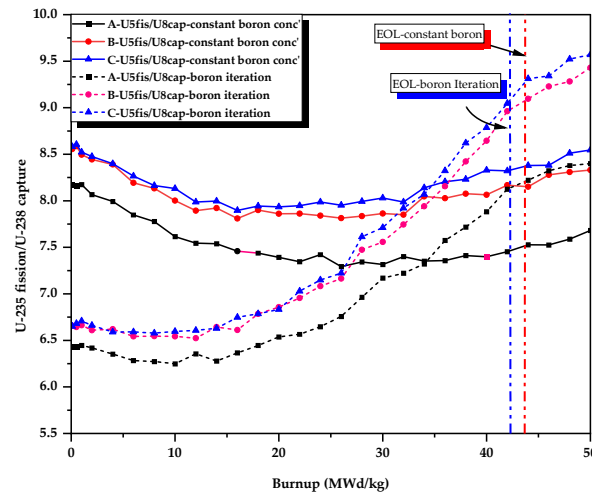


Figure 4. U-235 fission to U-238 capture ratio with burnup for boron iteration and constant boron concentration.

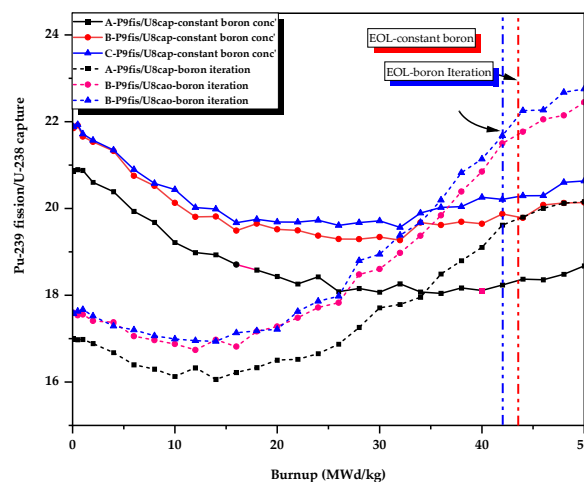


Figure 5. Variation with burnup of P9fis/U8cap spectral indices for boron iteration and constant boron concentration.

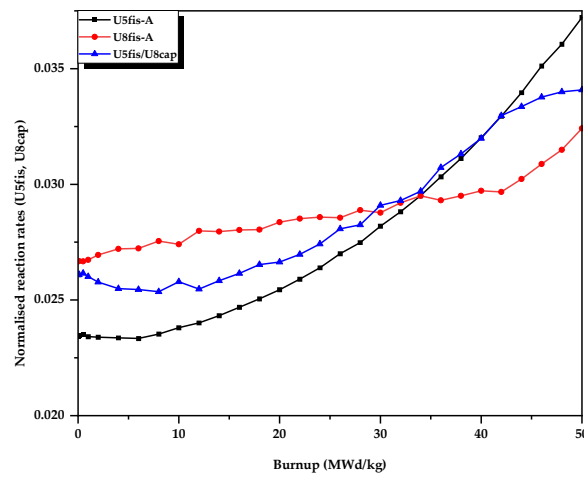


Figure 6. Variation with burnup of normalised U-235 fission reaction rate, U-238 capture reaction rate and U5fis/U8cap spectral indices for the boron iteration case.

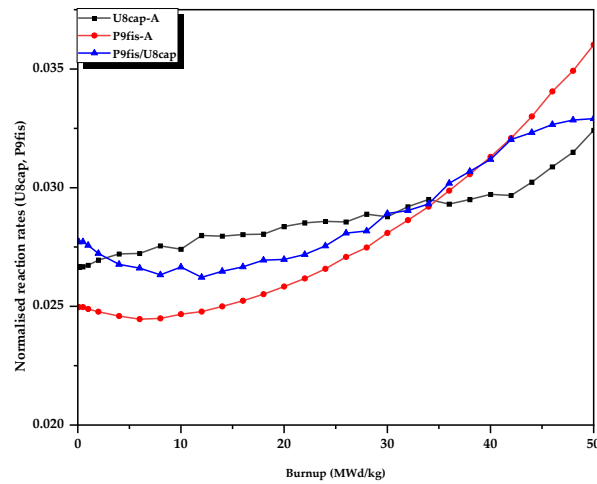


Figure 7. Variation with burnup of normalised Pu-239 fission and U-238 capture reaction rates and P9fis/U8cap spectral indices for the boron iteration case.

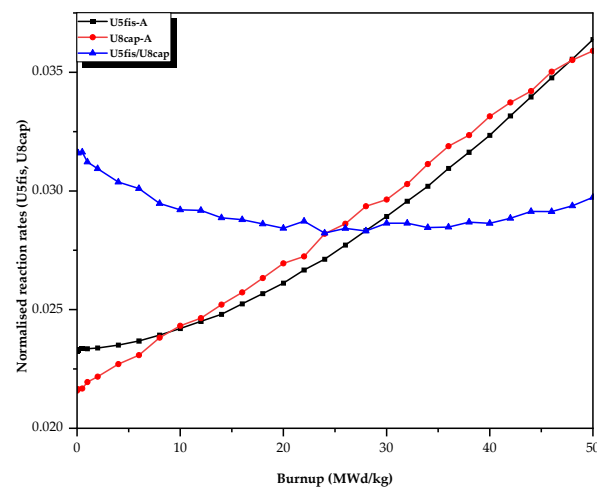


Figure 8. Variation with burnup of normalised U-235 fission and U-238 capture reaction rates and U5fis/U8cap spectral indices for the constant boron case.

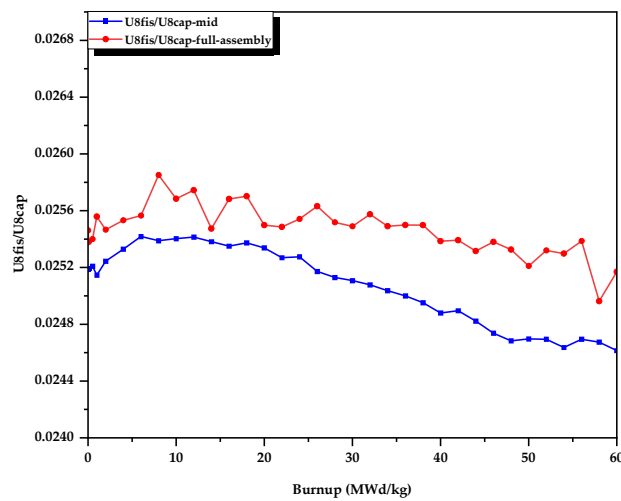


Figure 9. Variation with burnup of U_{8fis}/U_{8cap} spectral indices for the full assembly and mid-assembly horizontal segment with respect to boron iteration.

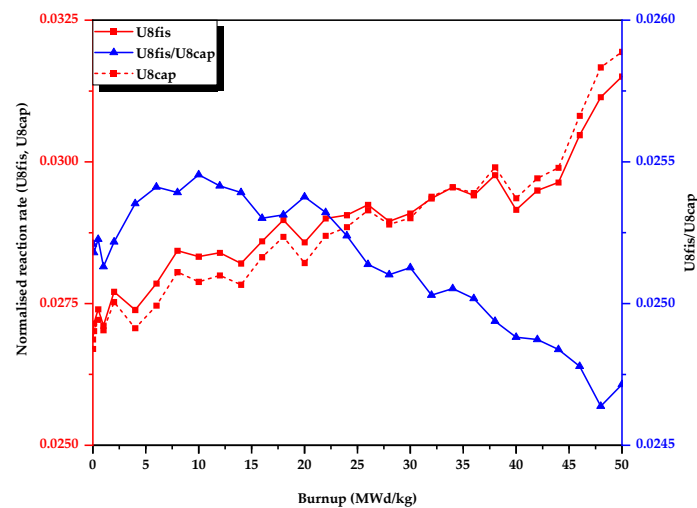


Figure 10. Normalised fission and capture reaction rates and fission to capture ratio with burnup for boron iteration middle assembly segment.

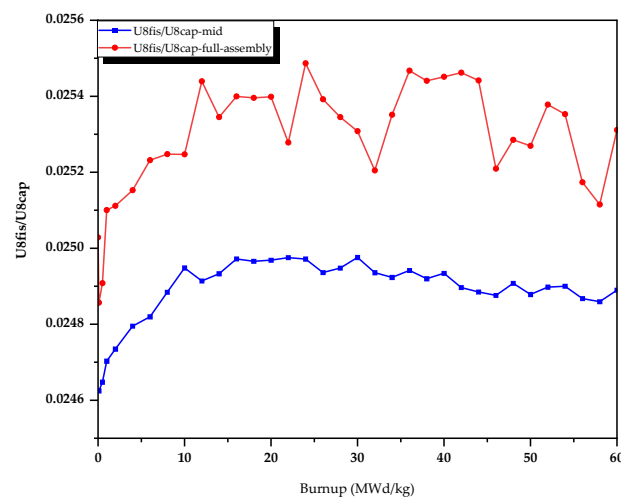


Figure 11. Variation with burnup of U_{8fis}/U_{8cap} spectral indices for the full assembly and mid-assembly horizontal segment with respect to constant boron.

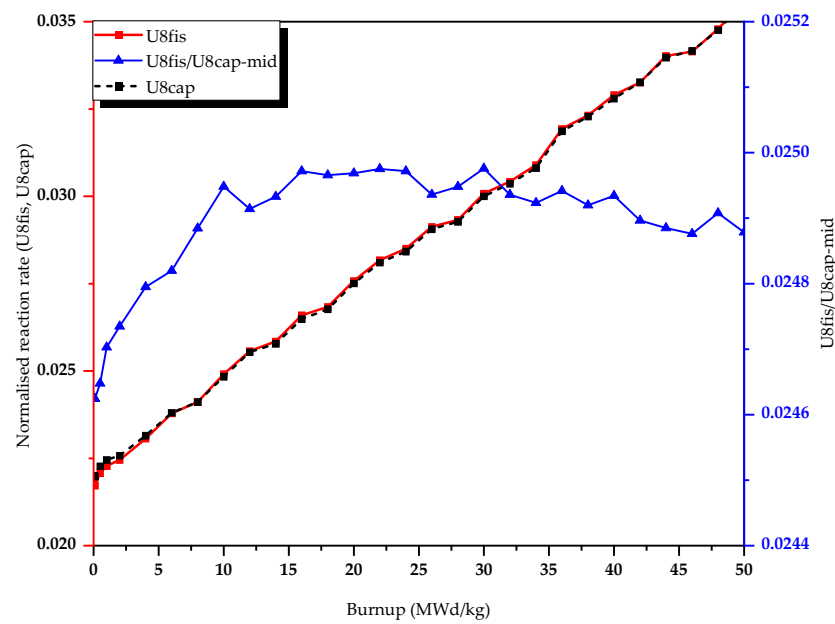


Figure 12. Normalised fission and capture reaction rates and fission to capture ratio with burnup for the constant boron middle assembly segment.

4.2. Analysis and Discussion

Figure 2 shows the boron let-down curve and constant boron criticality variation with burnup. The EOL burnup for Case-1 and Case-2 were determined to be 42 MWd/kg and 43.5 MWd/kg. The let-down curve gives an indication of the boron concentration required (at each burnup step) to hold down excess reactivity in such a way as to keep the reactor critical. The boron concentration at EOL for the assembly was determined to be 60 ppm. The constant boron criticality variation with burnup curve gives an indication of the effect of constant boron on EOL length. As can be observed, the constant boron case has an EOL length slightly greater compared to the boron iteration case.

Depletion calculations carried out relative to boron iteration take into account the combined effect of actual boron concentration and fuel depletion at each burnup step. The boron iteration method has the merit of adequate reactor core representation. However, using constant boron in depletion calculations and analysis of neutron spectrum behaviour would exaggerate the boron concentration requirements as burnup progresses. This is amplified in Figure 2 where the EOL length is increased due to increased excess reactivity hold-down.

A comparison of the neutron energy spectra for boron iteration and constant boron at BOL and EOL is presented in Figure 3. As observed from the graph, there is no energy peak shift in the fast region of the spectrum. The energy peak positions for BOL and EOL for boron iteration and constant boron cases are fixed. However, in the thermal region, a comparison of the energy peak positions at BOL and EOL spectra for the boron iteration case shows a spectral shift of about 0.025 eV to lower energies.

This spectral shift could be attributed to fuel depletion and reduction in boron concentration at EOL. The reduction in boron concentration reduces thermal neutron absorption causing thermal neutrons to live longer and accumulate at lower energies. The shift could also be caused by loss of both thermal and fast neutrons in the 'z' direction which is described with black boundary conditions. This type of loss in neutrons is known as diffusion cooling.

In the case of constant boron, the shift to lower energies was observed to be about 0.006 eV. The shift is minimal compared to the boron iteration case, as the concentration of boron remains at 1000 ppm at EOL. This high concentration of boron and the presence of neutron poisons in the fuel causes increased absorption of thermal neutrons thus the observed lower shift compared to the boron iteration case.

4.2.1. Neutron Flux at BOL

A comparison of the neutron flux for the boron iteration and the constant boron cases at BOL shows that in the fast and epithermal regions, the boron iteration case has a higher neutron flux compared to the constant boron case. The high neutron flux is due to the high boron concentration for the boron iteration case. High boron concentration implies an increase in thermal neutron absorption, thus leaving a high proportion of fast and epithermal neutrons, causing an increase in the fast and epithermal neutron flux.

In the thermal region, the opposite is observed where the constant boron case has a higher neutron flux compared to the boron iteration case. A high thermal neutron flux implies lower absorption of thermal neutrons resulting in increased thermal neutron population. The constant boron case has a lower boron concentration (1000 ppm) compared to the boron iteration concentration case (4000 ppm).

4.2.2. Neutron Flux at EOL

At EOL, the shift to lower energies for the constant boron case is smaller compared to the shift in the boron iteration case. This is caused by the difference in boron concentrations for the two cases at EOL. The constant boron case has a concentration of 1000 ppm, whereas the boron iteration case has 60 ppm. The high concentration of boron for the constant boron case and the presence of neutron poisons at EOL causes increased absorption of thermal neutrons thus the small shift to lower energies. However, the shift to lower energies for the boron iteration is higher because of the lower boron concentration of 60 ppm at EOL. The shift to lower energies in both cases could also be attributed *diffusion cooling* caused by increased leakage of fast neutrons in the 'z' direction which has black boundary conditions.

4.2.3. Spectral Indices

Figures 4 and 5 show changes in U_{5fis}/U_{8cap} and P_{9fis}/U_{8cap} spectral indices with burnup at locations A, B, and C, for boron iteration and constant boron cases.

With reference to the boron iteration case, it can be observed that from 0 MWd/kg to about 10 MWd/kg, there is a slight drop in spectral indices followed by an increase from 10 MWd/kg up to EOL. The small drop in spectral indices indicates a slight hardening of the spectrum. This is expected because of the high boron concentration at BOL. The high boron concentration absorbs thermal neutrons, thus increasing the importance of fast neutrons. To understand this behaviour, spectral indices were normalised to unit and the graphs are presented in Figures 6 and 7. Figure 6 compares normalised U-235 fission reaction rates, U-238 capture reaction rates, and associated U_{5fis}/U_{8cap} spectral indices for the boron iteration case at location 'A'. Figure 7 shows a comparison of normalised Pu-239 fission reaction rates, U-238 capture reaction rates, and associated P_{9fis}/U_{8cap} spectral indices for the boron iteration case at location 'A'. It can be observed from Figures 6 and 7 that the increase in the U-238 capture reaction rate is prominent compared to the fission reaction rates of U-235 and Pu-239.

The increase in the spectral indices from 10 MWd/kg to EOL is attributed to the rise in the U-235 and Pu-239 fission rates relative to the U-238 capture. This is expected as the importance of thermal neutrons increases due to a reduction in the boron concentration for the boron iteration case.

Unlike the boron iteration case, in the constant boron case, the drop in spectral indices observed in Figures 4 and 5 is more prominent up to about 30 MWd/kg, and then there is a slight increase up to EOL. This behaviour can be explained using Figure 8, which shows a variation with burnup of normalised U-235 fission, U-238 capture reaction rates and associated U_{5fis}/U_{8cap} spectral indices for the constant boron case at location 'A'. The drop in spectral indices from 0 MWd/kg to about 30 MWd/kg is due to the varying U-238 and U-235 reaction rates. The U-238 capture reaction rate has a linear increase with burnup, whereas the U-235 fission rate gradually increases exponentially. The slight increase in the spectral indices from 30 MWd/kg to EOL is due to the increasing importance of the U-235 fission reaction rate relative to the linear U-238 capture reaction rate. The slight

exponential growth in the U-235 fission reaction rate is associated with the slight increase in the number of neutrons reaching thermal energies towards EOL as discussed in Section 4.2.

Figure 9 shows changes with burnup of U8fis/U8cap spectral indices for the entire assembly treated as a detector and the mid-assembly sampled segment with respect to boron iteration. Both curves show an increase in spectral indices for the burnup range of 0 MWd/kg to 10 MWd/kg and a decrease from about 10 MWd/kg to EOL. However, there is an overall decrease in spectral indices for both cases, from 0.0255 to 0.0253 and 0.0252 to 0.0248, respectively. The observed hardening of the spectrum from 0 MWd/kg to about 10 MWd/kg is due to the high boron concentration at BOL. High boron concentrations cause an increase in thermal neutron absorption, thus making the spectrum hard or dominated by fast neutrons. The effect of fast neutrons can also be observed in Figure 10, where the importance of the U-238 fission reaction rate is greater compared to the U-238 capture reaction rate for the burnup range of 0 MWd/kg to 10 MWd/kg. The importance of the U-238 fission reaction rate is due to increased fast fission. The decrease in spectral indices is due to fuel depletion and a reduction in boron concentration. The reduction in boron concentration reduces the portion of fast neutrons and increases the population of thermal neutrons. As a result of this, there is a reduction in the fast fission of U-238 and hence the observed drop in spectral indices for both cases. A decrease in fast spectral indices indicates that the spectrum becomes softer with burnup.

Figure 11 compares the U8fis/U8cap spectral indices for the middle assembly segment and for the full assembly with respect to constant boron concentration. Both the middle segment and the full assembly spectral indices show an increase from 0 MWd/kg to around 15 MWd/kg. However, the full assembly shows poor detection statistics with a lot of fluctuations. The middle assembly spectral indices show improved detection statistics and shows a slight decrease in spectral indices which. This drop agrees with what was observed in Figure 9. Figure 12 presents the normalised U8fis/U8cap spectral indices for the constant boron case and associated normalised U8fis and U8cap reaction rates. The graph shows that there is minimal variation in importance of U8fis and U8cap reaction rates with burnup which makes the U8fis/U8cap spectral indices to have minimal variation with burnup. This makes it difficult to make conclusion on the status of the neutron spectrum with burnup.

The behaviour of the neutron spectrum with burnup as observed in the preceding discourse was carried out in the context of the thermal epi-thermal and fast regions of the neutron spectrum as well as the spectral indices. Leakage and absorption of neutrons was also considered during analysis. The perspective from which one discusses the neutron behaviour matters. If one discusses the neutron behaviour in the context of the thermal part of the neutron spectrum either for the boron iteration or constant boron cases, the softening of the spectrum is clear as there is a shift in energy peaks to lower energies. However, if one discusses the behaviour in the context of the fast region, one will conclude that there is no change in the spectrum with burnup as no shift in energy peaks is observe.

In trying to address the question; *Does the neutron spectrum in a PWR soften or harden with burnup?* It is important to be holistic in providing the response. The answer should be provided in the context of thermal and fast regions of the neutron spectrum, and spectral indices. The right model should be applied in trying to answer. The model should consider boron iteration and neutron leakage.

5. Conclusions

The behaviour of the neutron spectrum for a standard 3D, 17×17 fuel assembly was simulated using the Serpent Monte Carlo code. This was carried out to address the varying answers concerning the question; is the neutron spectrum harder or softer at EOL of a PWR reactor? An analysis of neutron spectra for the boron iteration and constant boron cases at BOL and EOL was performed. The results showed that there was a 0.025 eV and a 0.006 eV spectral shift to lower energies at EOL for the boron iteration and constant boron cases, respectively. This was an indication that the spectrum became softer with burnup. This was confirmed by an overall increase in thermal spectral indices (U5fis/U8cap and

P9fis/U8cap) with burnup. The softening of the spectrum was attributed to fuel depletion and reduction in boron concentration. Reduction in boron concentration reduced thermal neutron absorption and, as such, neutrons live longer and reach lower thermal energies, causing a pile-up and the observed spectral shift. Although the observed trends were similar, the boron interaction case's magnitude and spectral shift were more pronounced.

To summarise: Does the neutron spectrum in a PWR soften or harden with burnup?

The answer depends on the perspective. From the perspective of the thermal flux peak, the spectrum softens as function of burnup as the amount of boron is reduced to zero. This reduction in boron concentration, which is a strong absorption mechanism, is the main driver for that. From the perspective of the fast flux peak, the change is minor. The peak remains in the same energy range, as the neutrons born from fission are still born with similar energy levels. Therefore, if a question like this is posed, it is very important to understand the perspective from which it is asked.

Finally, the presented analysis in this paper provides an additional consideration in estimation of fuel behaviour as function of burnup. This is linked to the design of fuel with burnable absorbers inside. Although, not shown in this paper, the swing in the thermal flux peak will affect consumption of burnable poison, such as Gd_2O_3 . The impact may not be negligible; therefore, one should tread with care in such calculations. Therefore, proper models should be always preferred in carrying out irradiation analysis.

Author Contributions: This work was conceptualization by M.M.; the methodology was developed by both B.M.M. and M.M.; the simulations and analysis of the results were conducted by B.M.M.; the results and analysis were validated by M.M.; formal analysis, B.M.M.; investigation, B.M.M.; the original draft was prepared by B.M.M. and it was review and edited by M.M.; supervision of the work was conducted by M.M. All authors have read and agreed to the published version of the manuscript.

Funding: This work was partially sponsored by the International Atomic Energy Agency (IAEA), project number—ZAM-2020-003.

Data Availability Statement: The raw data supporting the conclusions of this article will be made available by the authors on request.

Acknowledgments: We would like to express gratitude to Paul Cosgrove from the University of Cambridge for agreeing to comment on and support this work. The Nuclear Energy MPhil course at the University of Cambridge is the inspiration for this work.

Conflicts of Interest: The authors declare no conflicts of interest. The funders had no role in the design of the study; in the collection, analyses, or interpretation of data; in the writing of the manuscript; or in the decision to publish the results.

Abbreviations

The following abbreviations are used in this manuscript:

BOL	Beginning of Life
EOL	End of Life
IAEA	International Atomic Energy Agency
LRM	Linear Reactivity Model
LWR	Light Water Reactor
PWR	Pressurised water Reactor
NFI	Nuclear Futures Institute

References

1. Hakim, A.R.; Harto, A.W.; Agung, A. Neutronic analysis of fuel assembly design in Small-PWR using uranium mononitride fully ceramic micro-encapsulated fuel using SCALE and Serpent codes. *Nucl. Eng. Technol.* **2019**, *51*, 1–12. [[CrossRef](#)]
2. Knief, R.A. *Theory and Technology of Commercial Nuclear Power*, 2nd ed.; American Nuclear Society: Downers Grove, IL, USA, 2014.
3. Ryu, K.H.; Shin, Y.-H.; Cho, J.; Hur, J.; Lee, T.H.; Park, J.-W.; Park, J.; Kang, B. Numerical investigation on the hydraulic loss correlation of ring-type spacer grids. *Nucl. Eng. Technol.* **2022**, *54*, 860–866. [[CrossRef](#)]

4. Mweetwa, B.M.; Ampomah-Amoako, E.; Akaho, E.H.K.; Odoi, C. Prediction of Neutronic and Kinetic Parameters of Ghana Research Reactor 1 (GHARR-1) after 19 Years of Operation Using Monte Carlo-N Particle (MCNP) Code. *World J. Nucl. Sci. Technol.* **2018**, *8*, 160–175. [[CrossRef](#)]
5. Kok, K.D. *Nuclear Engineering Handbook*; Taylor & Francis Group: Abingdon, UK, 2009.
6. Kerlin, T.W.; Upadhyaya, B.R. Fission product poisoning. In *Dynamics and Control of Nuclear Reactors*; Academic Press: Cambridge, MA, USA, 2019; pp. 57–71.
7. Wolniewicz, P.; Hellesen, C.; Håkansson, A.; Svärd, S.J.; Jansson, P.; Österlund, M. Detecting neutron spectrum perturbations due to coolant density changes in a small lead-cooled fast nuclear reactor. *Ann. Nucl. Energy* **2013**, *58*, 102–109. [[CrossRef](#)]
8. Şahin, S.; Khan, M.J.; Ahmed, R. Fissile fuel breeding and minor actinide transmutation in the life engine. *Fusion Eng. Des.* **2011**, *86*, 227–237. [[CrossRef](#)]
9. Stacey, W.M. *Nuclear Reactor Physics*; John Wiley & Sons: Hoboken, NJ, USA, 2007.
10. Lamarsh, R.J.; Anthony, J.B. *Introduction to Nuclear Engineering*, 3rd ed.; Prentice-Hall: Hoboken, NJ, USA, 2001.
11. Galahom, A.A. Simulate the effect of integral burnable absorber on the neutronic characteristics of a PWR assembly. *Nucl. Energy Technol.* **2018**, *4*, 287–293. [[CrossRef](#)]
12. International Atomic Energy Agency. IAEA-TECDOC-699, *Impact of Extended Burnup on the Nuclear Fuel Cycle, Proceedings of the Proceedings of an Advisory Group Meeting, Vienna, Austria, 2–5 December 1991*; International Atomic Energy Agency: Vienna, Austria, 1993.
13. Mustafa, S.S. Neutronic investigation of enriched gadolinium, natural gadolinium and Zirconium-erbium as burnable poisons in the advanced PWR assemblies by MCNPX code. *Radiat. Phys. Chem.* **2023**, *212*, 111129. [[CrossRef](#)]
14. Hanson, A.L.; Diamond, D.J. *Calculation of Kinetics Parameters for the NBSR*; Nuclear Science and Technology Department, Brookhaven National Laboratory: Upton, NY, USA, 2012.
15. Knott, D.; Yamamoto, A.; Cacuci, D.G. *Handbook of Nuclear Engineering-Reactor Design*; Springer Science+Business Media: New York, NY, USA, 2010. [[CrossRef](#)]
16. Lamarsh, J.R. *Introduction to Nuclear Reactor Theory*, 2nd ed.; Addison-Wesley: Reading, MA, USA, 1983.
17. Nabila, U.M.; Sahadath, H. Neutronic and fuel cycle performance of LEU fuel with different means of excess reactivity control: Impact of neutron leakage and refueling scheme. *Ann. Nucl. Energy* **2022**, *175*, 109245. [[CrossRef](#)]
18. Duderstadt, J.J.; Hamilton, L.J. *Nuclear Reactor Analysis*; Wiley: New Delhi, India, 2019.
19. Leppänen, J. *Serpent-a Continuous-Energy Monte Carlo Reactor Physics Burnup Calculation Code User's Manual*; VTT Technical Research Centre of Finland: Espoo, Finland, 2015.
20. Leppänen, J. Performance of Woodcock delta-tracking in lattice physics applications using the Serpent Monte Carlo reactor physics burnup calculation code. *Ann. Nucl. Energy* **2010**, *37*, 715–722. [[CrossRef](#)]
21. Coupled Neutronic/Thermal-Fluid Benchmark of the MHTGR-350 MW Core Design: Results for the Lattice Physics Exercises. 2020. Available online: https://oecd-nea.org/jcms/pl_46584/coupled-neutronic/thermal-fluid-benchmark-of-the-mhtgr-350-mw-core-design-results-for-the-lattice-physics-exercises (accessed on 14 December 2023).

Disclaimer/Publisher's Note: The statements, opinions and data contained in all publications are solely those of the individual author(s) and contributor(s) and not of MDPI and/or the editor(s). MDPI and/or the editor(s) disclaim responsibility for any injury to people or property resulting from any ideas, methods, instructions or products referred to in the content.